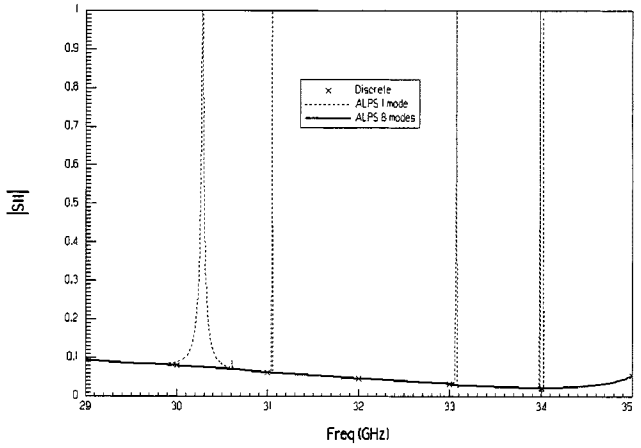

Fig. 10. Effect of not including all the propagating modes for Fig. 9.

peaks and, hence, realize the importance of including all the propagating modes when using the transfinite-element method.

Compared to the AWE, although the ALPS spends extra time on computing the eigenvectors of a tridiagonal matrix, it is not only more reliable, but overall more efficient, because it can tell the range of validity and, hence, terminate at earlier time. Its computational time depends on the number of poles inside the circle of convergence covering the interested band. Typically, four projecting vectors per pole are needed. The poles near the real axis influences the frequency response curve the most. It is unwise to ask for too big a frequency range because this will enclose a lot of unimportant poles in the circle of convergence. It is more efficient to break up a large band into a series of smaller bands. Since each band requires its own matrix inversion, this cost has to be balanced against the saving on the number of projecting vectors needed. When the sparse matrix decomposition is replaced by an iterative solver, the strategy will tilt toward more finer subdivisions of the band.

The limitation of current procedure lies on the assumption that higher order matrices of the polynomial matrix equation are relatively small. In the case of high lossy problem, the entries of higher order matrices may not be small. Numerical experiments show the procedure takes more iterations to converge. Also, (9) is no longer an appropriate approximation of system eigenvalues. One must compute the eigenvalues of the reduced system.

ACKNOWLEDGMENT

The authors would like to thank their colleague, Dr. R. Dyczij-Edlinger, Ansoft Corporation, Pittsburgh, PA, for his ingenious insight.

REFERENCES

[1] J. C. Nedelec, "Mixed finite elements in R3," *Numer. Math.*, vol. 35, pp. 315–341, 1980.
[2] Z. Cendes and J.-F. Lee, "The transfinite element method for modeling MMIC devices," *IEEE Trans. Microwave Theory Tech.*, vol. 36, pp. 1639–1649, Dec. 1988.
[3] X. Yuan and Z. Cendes, "A fast method for computing the spectral response of microwave devices over a broad bandwidth," in *Proc. IEEE AP-S/URSI Int. Symp. Dig.*, Ann Arbor, MI, June 1993, p. 196.
[4] L. T. Pillage and R. A. Rohrer, "Asymptotic waveform evaluation for timing analysis," *IEEE Trans. Computer-Aided Design*, vol. 9, pp. 352–366, Apr. 1990.
[5] P. Feldmann and R. W. Freund, "Efficient linear circuit analysis by Padé approximation via the Lanczos process," *IEEE Trans. Computer-Aided Design*, vol. 14, pp. 639–649, May 1995.
[6] D.-K. Sun, "ALPS—An adaptive Lanczos-Padé spectral solution of mixed-potential integral equation," in *USNC/URSI Radio Sci. Meeting Dig.*, July 1996, p. 30.
[7] D.-K. Sun, "ALPS—An adaptive Lanczos–Padé spectral solution of mixed-potential integral equation," *Comput. Methods Appl. Mech. Eng.*, vol. 169, pp. 425–432, 1999.
[8] C. Lanczos, "An iterative method for the solution of the eigenvalue problem of linear differential and integral operators," *J. Res. Natl. Bur. Stand.*, vol. 45, pp. 255–282, 1950.
[9] J. E. Bracken, D.-K. Sun, and Z. Cendes, "S-domain methods for simultaneous time and frequency characterization of electromagnetic devices," *IEEE Trans. Microwave Theory Tech.*, vol. 47, pp. 1277–1290, Sept. 1998.
[10] E. H. Newman, "Generation of wide-band data from the method of moments by interpolating the impedance matrix," *IEEE Antennas Propagat.*, vol. 30, pp. 1820–1824, Dec. 1988.
[11] B. N. Parlett and D. S. Scott, "The Lanczos algorithm with selective orthogonalization," *Math. Comput.*, vol. 33, no. 145, pp. 217–238, 1979.

Analysis and Design of Impedance-Transforming Planar Marchand Baluns

Kian Sen Ang and Ian D. Robertson

***Abstract*—A technique for designing impedance-transforming baluns is presented in this paper. It is based on the Marchand balun with two identical coupled lines. By varying the coupling factor of the coupled sections, a wide range of impedance transforming ratios can be achieved. In addition, a resistive network added between the balun outputs is proposed to achieve balun output matching and isolation. Microstrip baluns, matched at all ports, for transforming from a 50-Ω source impedance to 40-Ω as well as 160-Ω load terminations are realized to demonstrate the technique.**

***Index Terms*—Baluns, circuit analysis, couplers, impedance matching.**

I. INTRODUCTION

Baluns are key components in balanced circuit topologies such as double balanced mixers, push–pull amplifiers, and frequency doublers [1]–[3]. Various balun configurations have been reported for applications in microwave integrated circuits (MICs) and microwave monolithic integrated circuits (MMICs) [1]–[8]. Among them, the planar version of the Marchand balun [9] is perhaps one of the most attractive due to its planar structure and wide-band performance.

The planar Marchand balun consists of two coupled sections, which may be realized using microstrip coupled lines [5], Lange couplers [6], multilayer coupled structures [7], or spiral coils [8]. These baluns are usually designed through circuit simulations using full-wave electromagnetic analysis [1] or lumped-element models [8]. Various synthesis techniques using coupled-line equivalent-circuit models and analytically derived scattering parameters have also been reported [10], [11]. In this paper, the planar Marchand balun is analyzed as a combination

Manuscript received November 23, 1999. This work was supported by the Engineering and Physical Sciences Research Council. The work of K. S. Ang was supported by the Defence Science Organization National Laboratories.

The authors are with the Microwave and Systems Research Group, School of Electronic Engineering, Information Technology and Mathematics, University of Surrey, Guildford, Surrey GU2 7XH, U.K. (e-mail: k.ang@eim.surrey.ac.uk).

Publisher Item Identifier S 0018-9480(01)01088-2.

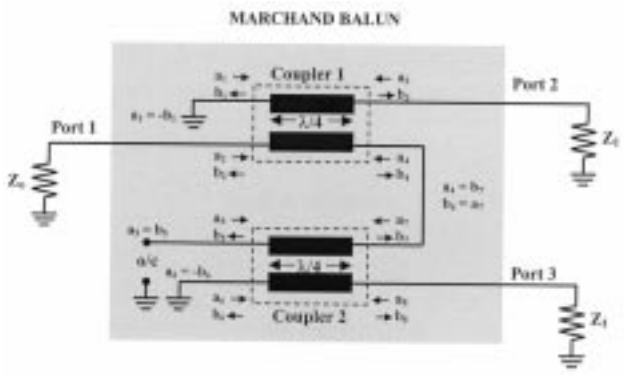

Fig. 1. Block diagram of a symmetrical Marchand balun as two identical couplers.

of two identical coupled sections. This simplifies the balun design to designing couplers with the appropriate coupling factor. This approach also provides valuable insight into the balun operation, relating the coupling factor of the coupler to the balun input and output impedances. This results in an effective technique for designing impedance-transforming baluns.

Most of the work on improving the planar Marchand balun has focused on achieving wide-band performance [1] and miniaturization [12]. The issue of balun output matching and isolation has not been addressed. This may be attributed to the well-known fact that a lossless reciprocal three-port network such as the balun cannot achieve perfect matching at all three ports. In many applications, however, balun output matching and isolation can enhance circuit performance. In double-balanced diode mixers, good output matching of the local oscillator (LO) and RF baluns at the diode interfaces can reduce LO power drive requirements and improve conversion loss. In push–pull amplifiers, isolation between the transistors provided by the balun outputs can enhance amplifier stability. In this paper, a resistive network connected between the balun outputs is proposed to achieve balun output matching and isolation. Combining this technique with impedance transforming Marchand baluns, a class of perfectly matched impedance-transforming baluns can be realized.

II. Analysis

A block diagram of the balun is shown in Fig. 1. It provides balanced outputs to load terminations Z_1 from an unbalanced input with source impedance Z_o. In general, the impedances Z_1 and Z_o are different. Balanced diode mixer applications, e.g., balanced signals, need to be fed to a pair of diodes whose impedance may differ from the 50-Ω source impedance. Thus, in addition to providing balanced outputs, the balun also needs to perform impedance transformation between the source and load impedances.

As shown in Fig. 1, the planar Marchand balun consists of two coupled sections, each of which is one quarter-wavelength long at the center frequency of operation. For symmetrical baluns, the scattering matrix of the balun can be derived from the scattering matrix of two identical couplers. We first consider the case where the source and load impedances are equal to Z_o. With the voltage waves defined in Fig. 1, the scattering matrix for ideal couplers with infinite directivity and coupling factor C is given by

$$[S]_{\text{coupler}} = \begin{bmatrix} 0 & C & -j\sqrt{1-C^2} & 0 \\ C & 0 & 0 & -j\sqrt{1-C^2} \\ -j\sqrt{1-C^2} & 0 & 0 & C \\ 0 & -j\sqrt{1-C^2} & C & 0 \end{bmatrix}. \tag{1}$$

The S-parameters of the balun can then be obtained by using the voltage wave's relationships indicated in Fig. 1, which has the form

$$[S]_{\text{balun}} = \begin{bmatrix} \dfrac{1-3C^2}{1+C^2} & j\dfrac{2C\sqrt{1-C^2}}{1+C^2} & -j\dfrac{2C\sqrt{1-C^2}}{1+C^2} \\ j\dfrac{2C\sqrt{1-C^2}}{1+C^2} & \dfrac{1-C^2}{1+C^2} & \dfrac{2C^2}{1+C^2} \\ -j\dfrac{2C\sqrt{1-C^2}}{1+C^2} & \dfrac{2C^2}{1+C^2} & \dfrac{1-C^2}{1+C^2} \end{bmatrix}. \tag{2}$$

When the balun load terminations are changed from Z_o to Z_1, as in Fig. 1, the balun S matrix of the balun has to be modified from $[S]_{\text{balun}}$ to $[S]'_{\text{balun}}$. The relationship between the two matrices are given by the following matrix equation:

$$[S]_{\text{balun}} = [A]^{-1}\Big([S]_{\text{balun}} - [\Gamma]^{+})([I] - [\Gamma][S]_{\text{balun}}\Big)^{-1}[A]^{+} \tag{3}$$

where $[I]$ is the identity matrix, while $[\Gamma]$ and $[A]$ are given by

$$[\Gamma] = \begin{bmatrix} 0 & 0 & 0 \\ 0 & \dfrac{Z_1 - Z_o}{Z_1 + Z_o} & 0 \\ 0 & 0 & \dfrac{Z_1 - Z_o}{Z_1 + Z_o} \end{bmatrix}$$

$$[A] = \begin{bmatrix} 0 & 0 & 0 \\ 0 & 2\dfrac{\sqrt{Z_1 Z_o}}{Z_1 + Z_o} & 0 \\ 0 & 0 & 2\dfrac{\sqrt{Z_1 Z_o}}{Z_1 + Z_o} \end{bmatrix}. \tag{4}$$

The S-parameters of the balun in Fig. 1 are then given by (5), shown at the bottom of the next page. Equation (5) shows that the use of identical coupled sections results in balun outputs of equal amplitude and opposite phase, regardless of the coupling factor and port terminations. To achieve optimum power transfer of -3 dB to each port, we require

$$|S'_{b,21}| = |S'_{b,31}| = \frac{1}{\sqrt{2}}. \tag{6}$$

With (5) and (6), the required coupling factor for optimum balun performance is given by

$$C = \frac{1}{\sqrt{\dfrac{2Z_1}{Z_o} + 1}}. \tag{7}$$

It is interesting to note that when all the ports are terminated with the same impedance, such as 50 Ω, where the impedance transforming ratio is unity, the required coupling factor is -4.8 dB and not -3 dB. Based on (5), the use of commonly assumed -3-dB couplers [6] will result in an insertion loss and output isolation of -3.5 dB and input and output return loss of -9.5 dB at the center frequency. When (7) is satisfied, the balun S matrix with parameters given by (5) reduces to

$$[S]_{\text{balun}} = \begin{bmatrix} 0 & \dfrac{j}{\sqrt{2}} & \dfrac{-j}{\sqrt{2}} \\ \dfrac{j}{\sqrt{2}} & \dfrac{1}{2} & \dfrac{1}{2} \\ \dfrac{-j}{\sqrt{2}} & \dfrac{1}{2} & \dfrac{1}{2} \end{bmatrix}. \tag{8}$$

This is the best attainable S matrix of a lossless balun. It is matched at the input and has transmission coefficients of -3 dB with oppo-

site phase. The outputs, however, are not matched or isolated. Both the output matching and isolation have a value of -6 dB.

To achieve perfect output port matching and isolation, some form of resistive network need to be added between the output ports, just as in the Wilkinson power divider. Y-parameters will be used to derive the required resistive network. The S matrix of a balun with perfect output matching and isolation has the form

$$[S]_{\text{balun}} = \begin{bmatrix} 0 & \frac{j}{\sqrt{2}} & \frac{-j}{\sqrt{2}} \\ \frac{j}{\sqrt{2}} & 0 & 0 \\ \frac{-j}{\sqrt{2}} & 0 & 0 \end{bmatrix}. \tag{9}$$

Based on the port terminations defined in Fig. 1, (9) can be converted to the Y matrix

$$[Y]_{\text{balun}} = \begin{bmatrix} 0 & \frac{-j}{\sqrt{2Z_oZ_1}} & \frac{j}{\sqrt{2Z_oZ_1}} \\ \frac{-j}{\sqrt{2Z_oZ_1}} & \frac{1}{2Z_1} & \frac{1}{2Z_1} \\ \frac{j}{\sqrt{2Z_oZ_1}} & \frac{1}{2Z_1} & \frac{1}{2Z_1} \end{bmatrix}. \tag{10}$$

Similarly, the S matrix of the symmetrical Marchand balun in (8) is converted to the Y matrix

$$[Y]_{\text{balun}} = \begin{bmatrix} 0 & \frac{-j}{\sqrt{2Z_oZ_1}} & \frac{j}{\sqrt{2Z_oZ_1}} \\ \frac{-j}{\sqrt{2Z_oZ_1}} & 0 & 0 \\ \frac{j}{\sqrt{2Z_oZ_1}} & 0 & 0 \end{bmatrix}. \tag{11}$$

Comparing (10) and (11), it can be deduced that the Y matrix of the resistive network has the form

$$[Y]_R = \frac{1}{2Z_1}\begin{bmatrix} 1 & 1 \\ 1 & 1 \end{bmatrix}. \tag{12}$$

This network can be realized by a series connection of a phase inverter and a resistor of value $2Z_1$. This resistive network can also be derived intuitively. The signal path between the two outputs is through the coupled ports of the two couplers, which has an attenuation of -6 dB with zero phase shift, as given by (8). Thus, by adding another signal path with -6-dB attenuation and 180° phase shift, perfect cancellation of the signal path between the outputs can be achieved.

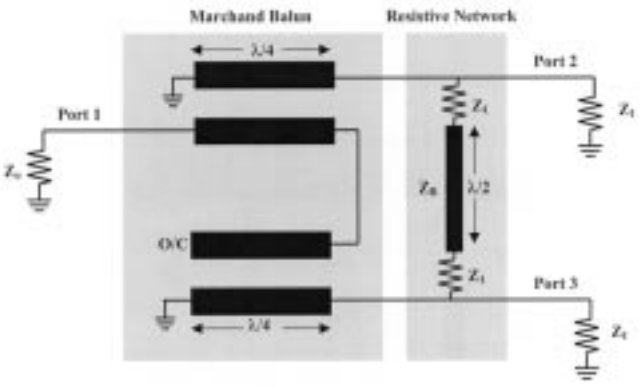

Fig. 2. Implementation of a perfectly matched balun with isolated outputs by adding a resistive network to the Marchand balun.

Fig. 2 shows the schematic diagram of the perfectly matched balun with the resistive network. The phase inverter is realized by a simple half-wavelength transmission line. To maintain symmetry between the output ports, the resistor is split into two resistors Z_1 at both ends of the transmission line. The performance of the resistive network is independent of the transmission-line characteristic impedance Z_R at the center frequency. However, Z_R should be set as high as possible to ensure that the operational bandwidth of the original balun is not significantly reduced. It should also be noted that the resistive network proposed could also be applied to other lossless balun structures to achieve output matching and isolation. In addition, the phase inverter in the resistive network can also be realized using other wide-band structures [13].

III. Experimental Results

To validate the analytical results and demonstrate the design approach, two perfectly matched impedance transforming baluns are designed. The first balun provides impedance transformation from 50 to 40 Ω, while the second balun provides impedance transformation from 50 to 160 Ω. These may represent requirements in balance diode mixers and multipliers [14], [3] for transforming between a 50-Ω source impedance and the diode impedances. The circuits are realized using microstrips, fabricated on a low-cost FR-4 board with a dielectric constant of 4.4 and thickness of 1.6 mm. For the 50–40-Ω impedance-transforming balun, Lange couplers were designed, fabricated, and measured to achieve the required coupling factor of -4.15 dB given by (7). A planar Marchand balun, consisting of two Lange couplers, was then fabricated. Microstrip lines with 50-Ω characteristic impedance were used to extend the three balun ports

$$[S]_{\text{balun}} = \begin{bmatrix} \frac{1-C^2\left(\frac{2Z_1}{Z_o}+1\right)}{1+C^2\left(\frac{2Z_1}{Z_o}-1\right)} & j\frac{2C\sqrt{1-C^2}\sqrt{\frac{Z_1}{Z_o}}}{1+C^2\left(\frac{2Z_1}{Z_o}-1\right)} & -j\frac{2C\sqrt{1-C^2}\sqrt{\frac{Z_1}{Z_o}}}{1+C^2\left(\frac{2Z_1}{Z_o}-1\right)} \\ j\frac{2C\sqrt{1-C^2}\sqrt{\frac{Z_1}{Z_o}}}{1+C^2\left(\frac{2Z_1}{Z_o}-1\right)} & \frac{1-C^2}{1+C^2\left(\frac{2Z_1}{Z_o}-1\right)} & j\frac{2C^2\left(\sqrt{\frac{Z_1}{Z_o}}\right)}{1+C^2\left(\frac{2Z_1}{Z_o}-1\right)} \\ -j\frac{2C\sqrt{1-C^2}\sqrt{\frac{Z_1}{Z_o}}}{1+C^2\left(\frac{2Z_1}{Z_o}-1\right)} & j\frac{2C\left(\frac{Z_1}{Z_o}\right)}{1+C^2\left(\frac{2Z_1}{Z_o}-1\right)} & \frac{1-C^2}{1+C^2\left(\frac{2Z_1}{Z_o}-1\right)} \end{bmatrix} \tag{5}$$

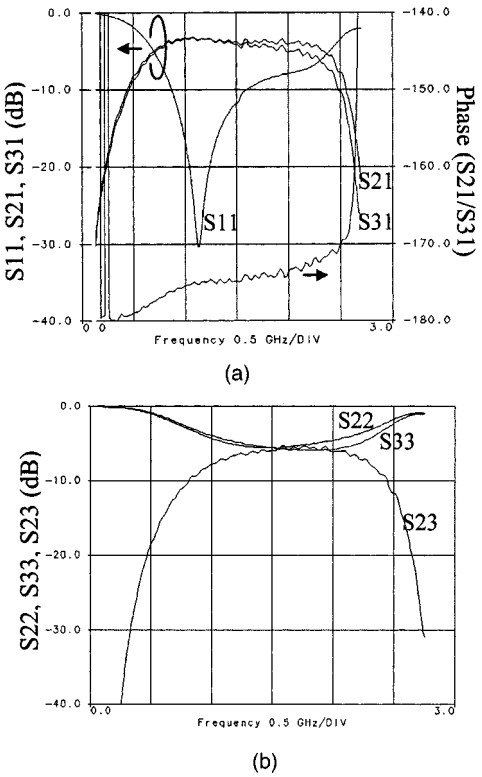

Fig. 3. Measured performance of 50–40-Ω impedance transforming balun without resistive network. Results are normalized to source and load impedances of 50 and 40 Ω, respectively. (a) Input return loss, insertion loss, and phase balance. (b) Output return loss and isolation.

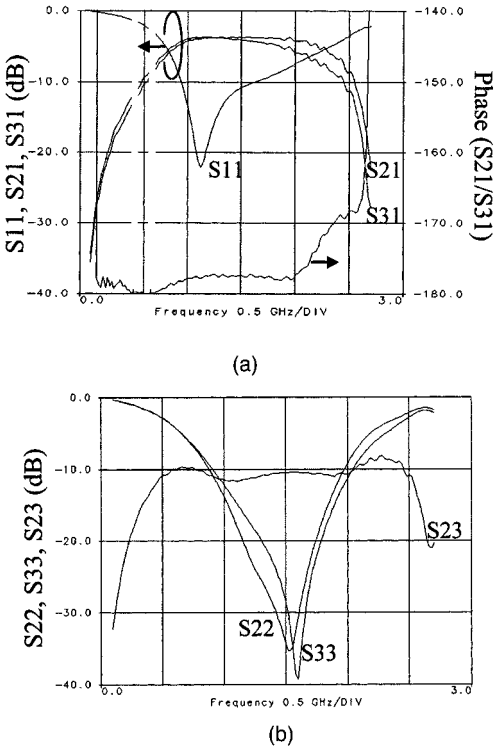

Fig. 4. Measured performance of 50–40-Ω impedance transforming balun with resistive network. Results are normalized to source and load impedances of 50 and 40 Ω, respectively. (a) Input return loss, insertion loss, and phase balance. (b) Output return loss and isolation.

to SMA connectors for measurement. A high-impedance half-wavelength transmission line is included between the output ports for implementation of the resistive network. Two chip resistors of 43 Ω were used for the resistive network.

The balun is measured, both with and without the resistive network. The balun is measured in a 50-Ω measurement system, two ports at a time, with the unused port terminated in a 50-Ω load. Deembedding is then performed to remove the effects of the 50-Ω microstrip lines between the balun ports and the SMA connectors. These 50-Ω-based S-parameters are then renormalized to the output impedance of 40 Ω using (3). The results obtained for the balun without the resistive network are given in Fig. 3(a) and (b). Fig. 3(a) shows that the balun input is well matched at about 1.2 GHz with a minimum insertion loss of −3.5 dB. The increasing amplitude imbalance at the high-frequency end of the passband can be attributed to the use of nonideal coupled sections with limited directivity. This is caused by the unequal even- and odd-mode phase velocities in the nonhomogeneous microstrip medium. These amplitude imbalances can be improved with the use of homogeneous dielectric mediums such as stripline. The phase balance between the outputs is within 10°. The balun output return loss and isolation is shown in Fig. 3(b). A minimum value of −6 dB is obtained for both the output return loss and isolation, which is in agreement with the theoretical results.

Fig. 4 shows the results obtained with the implementation of the resistive network. Comparing Figs. 3(a) and 4(a), the input matching and insertion loss of the balun remain essentially unchanged at mid-band, although the bandwidth is slightly reduced. The phase balance within the passband has improved to within 5°. Fig. 4(b) shows the balun output return loss and isolation. Good output matching at the coupler center frequency is now achieved. The output isolation has also improved to better than 10 dB within the passband.

The planar 50–160-Ω impedance-transforming balun is realized using two microstrip parallel coupled sections, which has a measured coupling factor of 8.8 dB at the center frequency of 2 GHz. A high-impedance half-wavelength transmission line is also included for implementation of the resistive network, which includes two 160-Ω chip resistors.

As in the previous balun, two-port measurements of the balun are performed, deembedded, and renormalized to the output impedance of 160 Ω. The measured performances are similar to the previous balun, except that it exhibits a smaller operational bandwidth due to the use of simple coupled line sections. The balun exhibits a well-matched input with −30-dB return loss and a minimum insertion loss of −3.5 dB. The phase balance is within 5°. Without the resistive network, the balun has poor output return loss and isolation, with values between 6–8 dB around the coupler center frequency. With the resistive network, the input matching and insertion losses remain unchanged, while the output port matching and isolation improved to better than −15 dB.

IV. Conclusion

This paper has demonstrated that impedance-transforming baluns can be realized using planar Marchand baluns with two identical coupled sections. Analytical results relating the impedance-transforming ratio to the coupling factor of the couplers have been presented. A technique for achieving output matching and isolation has also been proposed. These techniques have been verified through experimental results of two planar Marchand baluns employing Lange couplers and microstrip coupled lines. Perfectly matched baluns, transforming between a 50-Ω source impedance and load terminations of 40 and 160 Ω have been realized. This class of perfectly matched baluns with impedance

transformation capabilities is invaluable in the design of balanced microwave circuits such as mixers, push–pull amplifiers, and frequency doublers.

ACKNOWLEDGMENT

The authors would like to thank M. Blewett and D. Granger for their technical support in fabricating the circuits.

REFERENCES

[1] T. Chen *et al.*, "Broadband monolithic passive baluns and monolithic double balanced mixer," *IEEE Trans. Microwave Theory Tech.*, vol. 39, pp. 1980–1986, Dec. 1991.
[2] P. C. Hsu, C. Nguyen, and M. Kintis, "Uniplanar broad-band push–pull FET amplifiers," *IEEE Trans. Microwave Theory Tech.*, vol. 45, pp. 2150–2152, Dec. 1997.
[3] S. A. Maas and Y. Ryu, "A broadband, planar, monolithic resistive frequency doubler," in *IEEE Int. Microwave Symp. Dig.*, 1994, pp. 443–446.
[4] A. M. Pavio and A. Kikel, "A monolithic or hybrid broadband compensated balun," in *IEEE Int. Microwave Symp. Dig.*, 1990, pp. 483–486.
[5] W. R. Brinlee, A. M. Pavio, and K. R. Varian, "A novel planar double-balanced 6–18 GHz MMIC mixer," in *IEEE Microwave Millimeter-Wave Monolithic Circuit Symp. Dig.*, 1994, pp. 139–142.
[6] M. C. Tsai, "A new compact wide-band balun," in *IEEE Microwave and Millimeter Wave Monolithic Circuit Symp. Dig.*, 1993, pp. 123–125.
[7] K. Nishikawa, I. Toyoda, and T. Tokumitsu, "Compact and broad-band three-dimensional MMIC balun," *IEEE Trans. Microwave Theory Tech.*, vol. 47, pp. 96–98, Jan. 1999.
[8] Y. J. Yoon *et al.*, "Design and characterization of multilayer spiral transmission-line baluns," *IEEE Trans. Microwave Theory Tech.*, vol. 47, pp. 1841–1847, Sept. 1999.
[9] N. Marchand, "Transmission line conversion transformers," *Electronics*, vol. 17, no. 12, pp. 142–145, Dec. 1944.
[10] C. M. Tsai and K. C. Gupta, "A generalized model for coupled lines and its applications to two-layer planar circuits," *IEEE Trans. Microwave Theory Tech.*, vol. 40, pp. 2190–2099, Dec. 1992.
[11] R. Schwindt and C. Nguyen, "Computer-aided analysis and design of a planar multilayer Marchand balun," *IEEE Trans. Microwave Theory Tech.*, vol. 42, pp. 1429–1434, July 1994.
[12] R. H. Jansen, J. Jotzo, and R. Engels, "Improved compactions of a planar multilayer MMIC/MCM baluns using lumped element compensation," in *IEEE Int. Microwave Symp. Dig.*, 1997, pp. 227–280.
[13] T. Wang and K. Wu, "Size-reduction and band-broadening design technique of uniplanar hybrid coupler technique of uniplanar hybrid ring coupler using phase inverter for M(H)MIC's," *IEEE Trans. Microwave Theory Tech.*, vol. 47, pp. 198–206, Feb. 1999.
[14] S. A. Maas, *Microwave Mixers*, 2nd ed. Norwood, MA: Artech House, 1992.

A Novel Interpretation of Transistor S-Parameters by Poles and Zeros for RF IC Circuit Design

Shey-Shi Lu, Chin-Chun Meng, To-Wei Chen, and Hsiao-Chin Chen

***Abstract*—In this paper, we have developed an interpretation of transistor S-parameters by poles and zeros. The results from our proposed method agreed well with experimental data from GaAs FETs and Si MOSFET's. The concept of source-series feedback was employed to analyze a transistor circuit set up for the measurement of the S-parameters. Our method can describe the frequency responses of all transistor S-parameters very easily and the calculated S-parameters are scalable with device sizes. It was also found that the long-puzzled kink phenomenon of S_{22} observed in a Smith chart can be explained by the poles and zeros of S_{22}.**

***Index Terms*—Poles, S-parameters, transistors, zeros.**

I. INTRODUCTION

Wireless circuit design has recently become an important field all over the world. However, as far as RF circuit design is concerned, microwave circuit designers are talking about S-parameters, while analog circuit designers are thinking in terms of poles and zeros. Obviously, there is a gap between the thought processes of microwave circuit engineers and analog circuit engineers. For a long time, S-parameters have been understood in terms of Y- or Z-parameters. These Y- or Z-parameters, though very useful in calculating S-parameters, cannot give insight into the behaviors or physical meanings of S-parameters. For example, it is difficult for Y- or Z-parameters to describe the frequency responses of S-parameters directly or to explain the kink behavior of S_{22} observed in a Smith chart [1], such as the one shown in Fig. 1. In this paper, we present an interpretation of S-parameters from a poles' and zeros' point-of-view. By doing this, we can predict the frequency responses of S-parameters very easily and explain the kink behavior of S_{22} in Smith charts. Our calculated values of transistor S-parameters showed excellent agreement with the experimental data from 0.25-μm-gate Si MOSFETs and sub-micrometer gate GaAs FETs with different gate width.

II. THEORY

First, consider the circuit shown in Fig. 2(a), where an FET is connected for the measurement of its S-parameters. S_{11} and S_{21} can be measured by setting $V_2 = 0$ and $V_1 \neq 0$, while S_{22} and S_{12} can be measured by setting $V_1 = 0$ and $V_2 \neq 0$. Z_{O1} at input port and Z_{O2} at output port are both equal to 50 Ω, but are intentionally labeled differently. The reason for this will become clear later on. In general, the circuit in Fig. 2(a) is not easy to handle. However, the problem will be much easier to solve if this circuit is viewed as a dual feedback circuit, in which R_s is the local series–series feedback element and $C_{\rm gd}$ the local shunt–shunt feedback element. In order to simplify circuit analysis, we temporarily neglect the inductors and transform the circuit of Fig. 2(a) into that of Fig. 2(b) by using local series–series feedback

Manuscript received December 9, 1999. This work was supported under Grant 89-E-FA06-2-4, under Grant NSC89-2219-E-002-044, and under Grant NSC88-2219-E-005-003.

S.-S. Lu, T.-W. Chen, and H.-C. Chen are with the Department of Electrical Engineering, National Taiwan University, Taipei, Taiwan 10617, R.O.C. (e-mail: sslu@cc.ee.ntu.edu.tw).

C.-C. Meng is with the Department of Electrical Engineering, Chung-Hsing University, Taichung, Taiwan 40227, R.O.C.

Publisher Item Identifier S 0018-9480(01)01089-4.